Planetary and Space Science 65 (2012) 67–75

Contents lists available at SciVerse ScienceDirect

Planetary and Space Science

journal homepage: www.elsevier.com/locate/pss

Wave mechanism of the magnetospheric convection

A.S. Leonovich *

Institute of Solar-Terrestrial Physics SB RAS, P.O. Box 291, Irkutsk 664033, Russia

ARTICLE INFO

Article history:
Received 15 November 2011
Accepted 25 January 2012
Available online 7 February 2012

Keywords:
Magnetospheric convection
MHD-waves
Magnetosonic resonance
Quasilinear approximation

ABSTRACT

The problem of momentum transfer from the solar wind to the geotail via magnetosonic waves has been solved. The structure of the wave field of monochromatic MHD oscillations is calculated in a cylindrical model of the geotail with a background plasma distribution typical of the geotail lobes. Fast magnetosonic waves entering the magnetosphere from the magnetosheath excite slow magnetosonic waves at the resonance magnetic shells inside the geotail. Resonant oscillations interact with the background plasma transferring their momentum to it. The problem of modifying the ion distribution function of the background plasma for a given spectrum of magnetosonic oscillations in the magnetosheath has been solved in the quasilinear approximation. It is shown that, in the process, ions in the geotail lobes acquire an average Earthward velocity. The region of the most effective transfer of the momentum is near the magnetopause, in the area of open field lines, housing resonance shells for slow magnetosonic oscillations of a broad range of frequencies and wave numbers. The wave transfer mechanism for the momentum is capable of generating an Earthward flow of magnetospheric convection during prolonged periods of the Northern IMF component.

1. Introduction

Plasma convection in the magnetospheres of planets possessing their own magnetic field (including Earth), is a sufficiently complicated phenomenon. The structure of magnetospheric convection depends essentially on interplanetary magnetic field (IMF) orientation (Sergeev et al., 1996). In Earth's magnetosphere, convection is most intense during periods of Southern IMF component (Cowley, 1983). Notably, the plasma moves tailwards in regions adjacent to the magnetospheric boundary, while moving Earthwards in the inner regions, including the plasma sheet. The electric field of magnetospheric convection penetrates, along geomagnetic field lines, into the ionosphere where it is signature as convective cells of plasma motion in the polar cap and the auroral zone (Ruohoniemi and Baker, 1998). Magnetospheric convection is associated with the solar wind flowing around the magnetosphere, partially transferring its momentum to the magnetospheric plasma. Two main concepts have been proposed to explain the momentum transfer mechanism, which remain in use today.

The first concept was proposed by Dungey (1961). According to it, solar wind plasma enters the outer layers of the magnetosphere when geomagnetic field lines reconnect with interplanetary magnetic field lines in the frontal part of the magnetosphere, and are later transported into the geotail by the solar wind. This movement generates a tailward flow of magnetospheric convection. An inverse reconnection between the IMF and geomagnetic field lines occurs in the distant tail, where they become closed again. In the geotail plasma sheet, Earthward plasma motion is caused by the drift mechanism related to the dawn-dusk electric field resulting from solar wind plasma flowing around the magnetosphere. This model, involving the formation of two convection cells, agrees well with the behavior of the IMF components—magnetospheric convection increases when the Southern IMF component appears providing the conditions for effective reconnection between the geomagnetic field and IMF.

Unfortunately, this model cannot explain all the features of magnetospheric convection. For example, it does not fully explain magnetospheric convection in the absence of the Southern IMF component. During periods of the Northern IMF component, a new type of convective motion evolves in the magnetosphere—with three or four convective cells (Potemra et al., 1984; Forster et al., 2008). Two of these are the same cells as in the case of the Southern IMF component with decaying convective motion. Against their background, one or two new cells form in the region of open field lines (at geomagnetic latitudes above 75°). The direction of plasma motion in these cells is opposite to that in the first two cells (so-called "inverse convection"). To explain this phenomenon within the Dungey concept, the IMF and geomagnetic field lines are deemed to reconnect in high latitudes in the magnetospheric cusp in the presence of the B_y component in the IMF (Crooker et al., 1998; Sandholt et al., 2000). How these cells

* Tel.: +7 89148979925; fax: +7 83952511675.
E-mail address: leon@iszf.irk.ru

0032-0633/$ - see front matter © 2012 Elsevier Ltd. All rights reserved.
doi:10.1016/j.pss.2012.01.009

close via a convective Earthward flow in the region of open field lines still remains to be understood, however.

Another concept of magnetospheric convection has been proposed by Axford and Hines (1961). A mechanism has been suggested for the momentum transfer from the solar wind into the magnetosphere, similar to viscous interaction in liquids with shear flow. Such a type of plasma flow is realized at the magnetospheric boundary. This mechanism has been termed as 'quasi-viscous interaction'. The presence of such interaction in a collisionless plasma is also an assumption based on the turbulent nature of the flow around the magnetosphere (Miura, 1984; Mishin, 2005). If we accept this assumption, then, unlike the Dungey mechanism, the conditions for quasi-viscous interaction are always satisfied in the magnetosphere. The momentum transfer efficiency is mainly related to the solar wind speed.

That model cannot qualify as a complete description of magnetospheric convection, either. For example, it does not explain the dependence of the magnetospheric convection regime on the IMF orientation. Nor does it clarify the mechanism of the convection velocity changing its direction in the geotail (the Earthward and tailward flows of the convection are discussed separately). The issue of the above features of convection for the Northern IMF component remain unaddressed, too.

There is also an alternative point of view claiming that, vice versa, it is the flow existing in the plasma sheet (sustained by the plasma pressure gradient) that generates the convection electric field (Vasyliunas, 2001). This motion drags away plasma of closed field lines of the geotail, forming an Earthward flow of magnetospheric convection. The mechanism of magnetospheric convection is described in detail in Ponomarev et al. (2006), linking the momentum of the magnetospheric plasma to the electric field generated in the Bow shock front and penetrating into the magnetosphere.

There is, however, one more possibility of how the momentum may be transferred from the solar wind into the magnetosphere. The magnetosheath plasma flow is turbulent. Such plasma oscillations can be regarded as a stochastic flow of magnetosonic waves, partly directed towards the magnetosphere. Leonovich et al. (2003) have shown that up to 50 % of the energy of this wave flux can penetrate into the geotail. The integrated energy of the wave flux penetrating into the magnetosphere during a typical time interval between two successive substorms is the two orders of magnitude larger than the total energy of magnetospheric convection and can be used to maintain it. This is only a potential capacity, however.

Calculations in that paper referred to the simplest model medium consisting of two homogeneous half-spaces separated by a transition layer. The real magnetosphere is strongly inhomogeneous, and the geotail cross-section is spatially limited. For each harmonic of magnetosonic waves there is a surface in the magnetosphere from which it is completely reflected. Therefore, if no appreciable absorption of their energy takes place while magnetosonic oscillations travel from the magnetopause to the turning point, they must be reflected back into the solar wind in almost their entirety. Direct heating of the magnetospheric plasma by the solar wind MHD waves has been found to be rather ineffective (Kozlov, 2010). The energy of MHD oscillations is known to be efficiently absorbed at resonance surfaces for the Alfven and slow magnetosonic (SMS) waves (Leonovich and Kozlov, 2009). The SMS waves are especially interesting in this regard. Due to their very dissipative nature they are weakly localized across magnetic shells and can interact with ions of the bulk of the background plasma distribution function.

To check this possibility, we employ quasilinear theory to calculate the velocity the background plasma acquires when interacting with the flux of fast magnetosonic (FMS) waves penetrating into the magnetosphere from the magnetosheath. To this end, we will calculate the field structure of monochromatic MHD waves in a cylindrical model of the geotail where the plasma distribution is typical of the tail lobes. Specifying the FMS-wave spectrum in the magnetosheath and integrating over all harmonics, we will find the diffusion coefficient for plasma ions in the velocity space at each magnetic shell in the tail. Using the quasilinear theory equation for the ion distribution function, we will calculate the asymptotic distribution of their velocities across the geotail. We will determine the characteristic time the asymptotic regime takes to set in for each resonance shell.

This work has the following structure. Section 2 presents a cylindrical model of the geotail with a plasma distribution characteristic for its lobes. In Section 3, an equation is obtained describing the field of monochromatic MHD waves in this cylindrical model and the spatial structure of individual harmonics are computed. In Section 4, an equation is obtained describing, in the quasilinear approximation, the modification of the distribution function of plasma ions under the impact of SMS waves excited on the resonance magnetic shells by FMS waves penetrating into the geotail. Section 5 presents numerical computations of the asymptotic distribution (across the geotail) of the average velocity of plasma ions acquired under the impact of the FMS wave flux from the magnetosheath. Section 6 presents calculations of the distribution of the characteristic time needed for the asymptotic regime to set in on the resonance shells inside the tail and discusses the results. Section 7 lists the main results of this study.

2. Model of medium

Let us consider a model magnetotail in the form of an inhomogeneous plasma cylinder as shown in Figs. 1 and 2. The plasma distribution over radius corresponds to the geotail lobes. This model does not explicitly take into account the plasma sheet. Its presence is simulated by the radial distribution of the Alfven and SMS velocity. Moving away from the cylinder axis, they change from values characteristic of the plasma sheet to those typical of the geotail lobes. The radial distribution of the Alfven speed is plotted in Mazur and Leonovich (2006) based on satellite data for the distribution of plasma concentration and magnetic field in the magnetosphere (Sergeev and Tsyganenko, 1980; Borovsky et al., 1998). Since the main results of

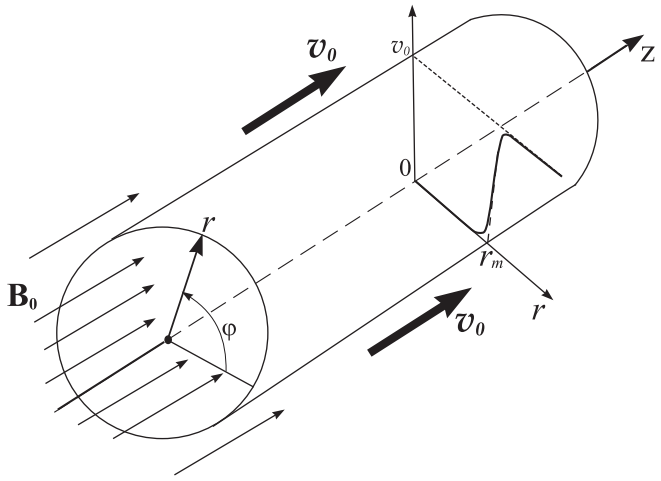

Fig. 1. A cylindrical model of the magnetotail within the solar wind plasma flow. Magnetic field $\mathbf{B_0}$ is along the plasma cylinder axis. The radial distribution of the solar wind velocity v_0 flowing round the geotail is shown schematically.

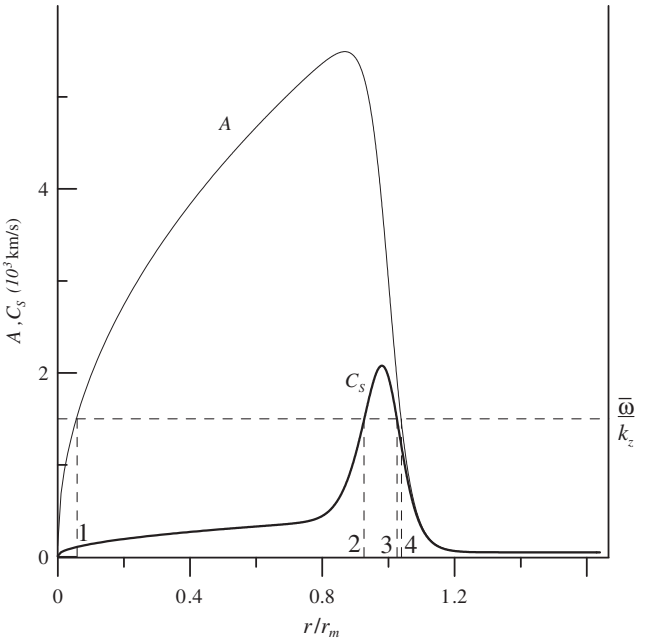

Fig. 2. Distribution of the Alfven speed $A(r)$ and velocities of SMS waves $C_S(r)$ in the magnetotail and in the solar wind. On the resonance shells $r=r_S$ (points 2 and 3) and $r=r_A$ (points 1 and 4) the parallel phase velocity $\overline{\omega}/k_z$ of a monochromatic wave is equal, respectively, to local velocity C_S of SMS waves and Alfven speed A.

that study concern the region of open field lines, the presence of plasma sheet should not be an essential element in the calculations.

We introduce a cylindrical coordinate system (r,ϕ,z) in which the origin $r=0$ coincides with the axis of the plasma cylinder. The background magnetic field is directed along the z-axis. We assume that plasma in the magnetosheath moves along the z-axis at velocity v_0, while plasma is motionless in the geotail, in the absence of waves (see Fig. 1). Transition from the magnetospheric parameters to the magnetosheath parameters occurs in a narrow transition layer of thickness $\Delta_r \ll r_m$, where r_m is the characteristic radius of the geotail. We set such a plasma density distribution over the radius that its maximum is reached on the axis of the plasma cylinder falling to a minimum toward its boundary. Magnetic field in the magnetotail is stronger than in the solar wind. The distribution of the Alfven speed $A=B_0/\sqrt{4\pi\rho_0}$ over the radius is presented in Fig. 2. Such a distribution is typical for plasma parameters in the geotail lobes.

To describe perturbations in such a plasma configuration, we used a system of ideal MHD equations of the form

$$\rho\frac{d\overline{\mathbf{v}}}{dt}=\nabla\overline{P}+\frac{1}{4\pi}[\mathrm{curl}\overline{\mathbf{B}}\times\overline{\mathbf{B}}], \tag{1}$$

$$\frac{\partial\overline{\mathbf{B}}}{\partial t}=\mathrm{curl}[\overline{\mathbf{v}}\times\overline{\mathbf{B}}], \tag{2}$$

$$\frac{\partial\overline{\rho}}{\partial t}+\nabla(\rho\overline{\mathbf{v}})=0, \tag{3}$$

$$\frac{d}{dt}\frac{\overline{P}}{\overline{\rho}^{\gamma}}=0, \tag{4}$$

where $\overline{\mathbf{B}}$, $\overline{\mathbf{v}}$ are magnetic field and plasma velocity vectors, $\overline{\rho}$, $\overline{P}$ are the plasma density and pressure, $\gamma=5/3$ is the adiabatic index. Let us assume wave-related disturbances to be rather weak, so as to allow the initial system of Eqs. (1)–(4) to be linearized. Let us subscript the parameters linked to background plasma with zero, while using the unsubscripted values to denote the wave-related parameters ($\overline{\rho}=\rho_0+\rho$, $\overline{P}=P_0+P$, $\overline{\mathbf{B}}=\mathbf{B_0}+\mathbf{B}$, $\overline{\mathbf{v}}=\mathbf{v_0}+\mathbf{v}$). In the zero approximation, the r-component of Eq. (1) yields, in steady state ($\partial/\partial t=0$), the equilibrium condition of the plasma configuration

$$P_0+\frac{B_0^2}{8\pi}=const, \tag{5}$$

which defines the equilibrium distribution of plasma pressure $P_0(r)$ for a given distribution of $B_0(r)$. This pressure determines the distribution of sound velocity in plasma $S=\sqrt{\gamma P_0/\rho_0}$ and the corresponding velocity distribution of SMS waves $C_S=AS/\sqrt{A^2+S^2}$ in Fig. 2. We assume that magnetic field is almost constant both inside and outside the plasma cylinder, changing only in a thin transition layer of thickness $\Delta_r \ll r_m$. Our numerical computations used the following values $r_m=30\mathrm{Re}$, $\Delta_r=2\mathrm{Re}$, where $\mathrm{Re}=6370$ km is the average Earth radius. It follows from the equilibrium condition (5) that plasma pressure also varies in the transition layer only. Table 1 lists the values of the key parameters of the plasma and magnetic field on the geotail boundary used in the following computations. These parameters provide for the equilibrium condition (5) to be met in the plasma configuration.

Table 1
The main parameters of the medium on the geotail boundary.

Parameter	Geotail lobes	Magnetosheath
B_0 (nT)	20	5
A (km/s)	6000	50
S (km/s)	420	177
$\beta^*=S^2/A^2$	0.005	12.6

3. Structure of monochromatic MHD waves

Let us define the spatial structure of a monochromatic MHD wave in the geotail model under consideration. Denote the component of the disturbed vector of plasma velocity in the wave in the r-axis direction as $v_r=d\zeta/dt=\partial\zeta/\partial t+(\mathbf{v_0}\nabla)\zeta$, where ζ is the displacement of a plasma element. Consider a monochromatic wave of the form $\exp(ik_z z+im\phi-i\omega t)$, where k_z is the component of the wave vector in the z-axis direction, $m=0,1,2,3\ldots$ is the azimuthal wave number, ω is wave frequency. Linearizing the system of Eqs. (1)–(4) and expressing the other components of the oscillation field through ζ, we obtain (see Leonovich, 2011a)

$$v_r=-i\overline{\omega}\zeta,\quad v_\phi=-\frac{1}{K_S^2}\left(A^2+\frac{K_A^2S^2}{\chi_S^2}\right)\frac{m}{\overline{\omega}r^2}\frac{\partial r\zeta}{\partial r},$$
$$v_z=-\frac{k_zK_A^2S^2}{\overline{\omega}\chi_S^2 r}\frac{\partial r\zeta}{\partial r}-\zeta\frac{dv_0}{dr}, \tag{6}$$

$$B_r=ik_zB_0\zeta,\quad B_\phi=-\frac{k_zB_0}{\overline{\omega}}v_\phi,$$
$$B_z=-\frac{K_A^2B_0}{\chi_S^2}\left(1-\frac{k_z^2S^2}{\overline{\omega}^2}\right)\frac{1}{r}\frac{\partial r\zeta}{\partial r}-\zeta\frac{dB_0}{dr}, \tag{7}$$

$$P=-\gamma P_0\frac{K_A^2}{\chi_S^2}\frac{1}{r}\frac{\partial r\zeta}{\partial r}+\zeta\frac{d}{dr}\left(\frac{B_0^2}{8\pi}\right), \tag{8}$$

where

$$K_A^2=1-\frac{k_z^2A^2}{\overline{\omega}^2},\quad K_S^2=K_A^2-\frac{m^2A^2}{r^2\overline{\omega}^2},$$

$$\chi_S^2=K_S^2-K_A^2\frac{k_z^2+m^2/r^2}{\overline{\omega}^2}S^2,$$

$\overline{\omega}=\omega-k_z v_0$ is Doppler-modified oscillation frequency. For displacement ζ we obtain the equation

$$\frac{\partial}{\partial r}\ \frac{\rho_0\Omega^2}{k_r^2}\ \frac{1}{r}\frac{\partial r\zeta}{\partial r}+\rho_0\Omega^2\zeta=0, \tag{9}$$

where $\Omega^2=\overline{\omega}^2-k_z^2A^2$,

$$\begin{aligned}k_r^2&=\frac{\overline{\omega}^4}{\overline{\omega}^2(A^2+S^2)-k_z^2A^2S^2}-k_z^2-\frac{m^2}{r^2}\\&=k_z^2\left(\frac{\overline{\omega}_A^4/(1+\beta^*)}{(\overline{\omega}_A^2-\overline{\omega}_S^2)}-1-\frac{m^2}{k_z^2r^2}\right)\\&=\frac{k_z^2}{1+\beta^*}\frac{(\overline{\omega}_A^2-\overline{\omega}_{A1}^2)(\overline{\omega}_A^2-\overline{\omega}_{A2}^2)}{(\overline{\omega}_A^2-\overline{\omega}_S^2)},\end{aligned} \tag{10}$$

and $\overline{\omega}_A=\overline{\omega}/k_zA(r)$, $\overline{\omega}_S=\sqrt{\beta^*/(1+\beta^*)}$, $\beta^*=S^2/A^2$, and $\overline{\omega}_{A1}^2,\overline{\omega}_{A2}^2$ are the roots of biquadratic (with respect to $\overline{\omega}_A$) equation $k_r^2=0$. Note that the expression β^* coincides, up to a factor close to unity, with the known parameter $\beta=8\pi P_0/B_0^2$—the gas-kinetic plasma pressure to magnetic pressure ratio. From (9) it is evident that k_r^2 is the square of the r-component of the MHD wave-vector in the WKB approximation when solution of Eq. (9) can be presented as $\zeta\sim\exp(i\int k_r dr)$.

The turning points are determined by the zeros of the $k_r^2(r)$ function, and the resonance surfaces by the singular points of Eq. (9), in which the coefficient at the higher derivative becomes zero. At the Alfven resonance point $r=r_A$ we have $\Omega^2(r_A)=0$. At the magnetosonic resonance point $r=r_S$ the denominator in expression (10) becomes zero yielding the local dispersion equation for SMS waves when $|k_r^2|\to\infty:\overline{\omega}^2=k_z^2C_S^2(r_S)$. On the resonance surfaces the phase velocity in the magnetic field direction $\overline{\omega}/k_z$ of the MHD wave under study coincides with the local velocity of the Alfven or SMS wave (see Fig. 2). The following boundary conditions were used in the numerical solution of Eq. (9). When $r\to0$, a solution limited in amplitude was chosen to Eq. (9), which at $r\to0$ could be presented approximately as

$$r^2\zeta''+\sigma r\zeta'+(k_{r0}^2r^2-2+\sigma)\zeta=0,$$

where $k_{r0}^2\equiv k_r^2(r\to0)$ (for $m\neq0$ we have $k_{r0}^2\approx-m^2/r^2$). Here $\sigma=1$ for $m=0$ and $\sigma=3$ for $m\neq0$. The solution that is finite for $r\to0$ has the form

$$\zeta=C\begin{cases}r & \text{for } m=0,\\ r^{m-1} & \text{for } m\neq0,\end{cases}$$

where C is an arbitrary constant. The second boundary condition was formulated in the magnetosheath, at $r=2r_m$. It requires that the oscillation amplitude here is equated with the amplitude of the harmonic of FMS wave model spectrum in the magnetosheath (see Section 6), which determines the C constant and the oscillation amplitude in the entire space.

Moreover, to regularize singularities in (9), the expressions for the oscillation frequency have been redefined in the definition of Ω^2 and in the denominator for k_r^2 by adding imaginary parts that take into account dissipation of the Alfven and SMS oscillations at the resonance surfaces. The definition of Ω^2 assumed $\overline{\omega}=\omega-k_zv_0+i\gamma_A$, while $\overline{\omega}=\omega-k_zv_0+i\gamma_S$ in the denominator of (10), where $\gamma_{A,S}$ are decrements of the Alfven and SMS waves, respectively. The decrements determine the amplitude and characteristic scale of Alfven and SMS wave localization at the resonance shells. For the Alfven waves the decrement is small ($\gamma_A\sim10^{-3}\omega$), implying a large amplitude of resonant oscillations and a narrow area of their localization over the radius. The decrement of SMS waves strongly depends on the ion to electron temperature ratio in plasma (see Leonovich and Kozlov, 2009). In the solar wind the plasma electrons are hotter than the ions ($T_e\approx3T_i$), therefore, in the magnetosheath we assume $\overline{\gamma}_S\approx10^{-2}\omega$. In the tail lobes, on the contrary, plasma ions are hotter than the electrons ($T_i\approx8T_e$), which corresponds to $\overline{\gamma}_S\approx0.8\omega$. The decrement of SMS waves chosen for the magnetosheath changes to the one typical of the magnetosphere in the same transition layer as the other plasma parameters.

Consider the structure of the solution to (9) near the resonance surface $r=r_S$. Let us linearize the coefficient at the higher derivative in (9), expressing $k_r^{-2}\approx a_S^2\xi_S$, where $\xi_S=(r-r_S)/a_S$, $a_S=(-\partial k_r^{-2}/\partial r)_{r=r_S}$ is the characteristic scale of k_r^{-2} near $r=r_S$. Then Eq. (9) near $r=r_S$ can be presented as

$$\frac{\partial}{\partial\xi_S}(\xi_S+i\varepsilon_S)\frac{\partial\zeta}{\partial\xi_S}-\zeta=0, \tag{11}$$

where $\varepsilon_S=ma_S\gamma_S/k_zr_SC_S(r_S)$ is the regularized factor determined by the decrement of SMS waves. It should be taken into account that away from the resonance surface the SMS wave transforms into an almost undamped FMS wave. Therefore, the following model was used for the SMS wave decrement: $\gamma_S=\overline{\gamma}_S\exp[-(r-r_S)^2/\Delta_S^2]$ where $\Delta_S=a_S\beta^*/(1+(m/k_zr_S)^2)$ is the localization scale for which the oscillation field can be regarded as a resonant SMS wave (see Leonovich and Kozlov, 2009). The solution of (11) is

$$\zeta=C_1I_0(2\sqrt{\xi_S+i\varepsilon_S})+C_2K_0(2\sqrt{\xi_S+i\varepsilon_S}),$$

where $I_0(z),K_0(z)$ are modified Bessel functions, $C_{1,2}$ are arbitrary constants determined from the boundary conditions away from the resonance surface. It is evident that when $r\to r_S$ there is a solution with a logarithmic singularity

$$\zeta=-\frac{C_2}{2}\ln(\xi_S+i\varepsilon_S),$$

which corresponds to the resonant SMS wave.

Fig. 3 shows the radial structure of two monochromatic harmonics. There are resonance surfaces for SMS waves in the magnetosphere (Fig. 3a) for one of them, but not for the other (Fig. 3b). This figure presents the unity-normalized structure of the derivative $d\zeta/dz$ determining the maximum oscillation amplitude on the resonance surfaces. The resonance surfaces for the SMS wave are determined by the intersection points of functions $\mathrm{Re}(\overline{\omega}_A(r))$ and $\overline{\omega}_S(r)$, where the real part of the denominator in (10) vanishes.

4. Equation for ion distribution function in quasilinear approximation

Consider the problem of the ion distribution function in magnetospheric plasma transformed under the impact of the MHD wave flux from the magnetosheath. We use kinetic theory equations in the locally quasilinear approximation. This means that, on each resonance shell inside the geotail, we will consider the distribution function in the same way as if it were defined over the entire space, while assuming the MHD oscillation field to correspond to this shell. We assume the plasma to consist of the hydrogen ions and electrons. The equation for the ion distribution function in the presence of MHD waves with linear dispersion (such as the Alfven wave with $\omega=k_\parallel A$ or the SMS wave with dispersion law $\omega\approx k_\parallel C_S$) has the form (see Akhiezer et al., 1979)

$$\begin{aligned}\frac{\partial f}{\partial t}=&\left(\frac{e}{m_i}\right)^2\frac{\partial}{\partial v_\parallel}\int d^3\mathbf{k}\left[E_3J_0(\lambda)+i\frac{k_\parallel v_\perp}{\omega}J_0'(\lambda)E_2\right]^*\\&\times\int_0^t\left[E_3(t')J_0(\lambda)+i\frac{k_\parallel v_\perp}{\omega}J_0'(\lambda)E_2(t')\right]\frac{\partial f(t')}{\partial v_\parallel}e^{i(k_\parallel v_\parallel-\omega)(t-t')}\,dt'.\end{aligned} \tag{12}$$

Here, $f(v_\parallel,v_\perp,t)$ is the ion distribution function over velocities, $v_{\parallel,\perp}$ are ion velocities along and across magnetic field lines, $J_0(\lambda)$ is the Bessel function, $\lambda=k_\perp v_\perp/\omega_i$, $k_\parallel$, $\mathbf{k}_\perp$ are the parallel and the

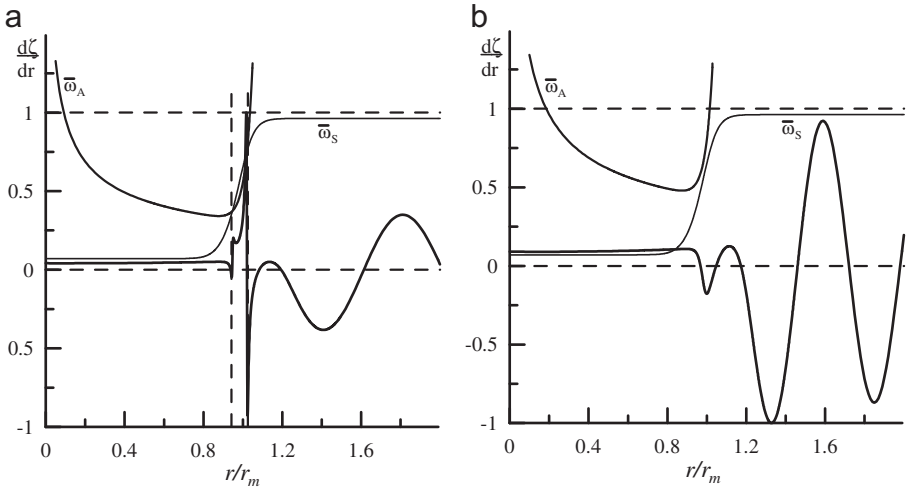

Fig. 3. The spatial structure of monochromatic MHD waves for azimuthal harmonic $m=1$ with different values of parallel phase velocity $\overline{\omega}/k_z$: (a) oscillations for which there are resonance shells for SMS-waves in the geotail ($\overline{\omega}_A(r_S)=\overline{\omega}_S(r_S)$) and (b) oscillations with no resonance shells inside the geotail.

perpendicular wave vector components, ω_i is ion gyrofrequency, and the various components of field oscillations are subscripted with $i=1,2,3$: $E_3\equiv\langle E_\parallel\rangle$ is the averaged amplitude of the oscillation electric field along the magnetic field after averaging over the wave number spectrum, E_1 is the average amplitude of the field along $\mathbf{k}_\perp$, and E_2 is the average amplitude along the vector $[\mathbf{B}_0\mathbf{k}_\perp]$. The relationship between the oscillation frequency and the wave vector components is determined by the local dispersion equation. Integration in (12) is with respect to the three components of the wave vector and the entire interval of time preceding the present moment. That is, in the general case, this equation is not local in time.

To solve this equation in its general form is rather a difficult problem. Here, we address a simpler problem of determining the asymptotic form of the distribution function when $t\to\infty$. The main contribution to the integral over t' in (12) is by asymptotic values E_i (since the source is a constant oscillation field in the magnetosheath, these values remain unchanged throughout the time interval in question), the distribution function f changing little on the asymptotics. Taking the functions E_i and f at $t'\to t$ outside the integral over t' in (12), we obtain the following equation (Sizonenko and Stepanov, 1968):

$$\frac{\partial f}{\partial t}\approx\frac{\partial}{\partial v_\parallel}D\frac{\partial f}{\partial v_\parallel},\tag{13}$$

where

$$D=\pi\left(\frac{e}{m_i}\right)^2\int d^3\mathbf{k}\left|E_3J_0(\lambda)+i\frac{k_\parallel v_\perp}{\omega}J_0'(\lambda)E_2\right|^2\delta(\omega-k_\parallel v_\parallel)$$

is the ion diffusion coefficient in the velocity space. Thus, it is clear that coupling occurs when the parallel wave phase velocity $\omega/k_\parallel$ is the same as the parallel plasma ion velocity $v_\parallel$.

Since the equation for the distribution function is obtained in the Cartesian coordinates, it is necessary to transform it for the cylindrical model we use for the geotail. The relationship between the electric and magnetic field components is determined by the equation $\mathbf{B}=-ic[\nabla\mathbf{E}]/\omega$. In the ideal MHD approximation, $E_3=0$ for all types of MHD waves, while for the E_2 component we have

$$E_2=\left\langle-\frac{\omega}{k_zc}\frac{k_r\tilde{B}_r+k_\phi\tilde{B}_\phi}{k_\perp}\right\rangle,$$

the angular brackets $\langle\rangle$ denote averaging over the wave vector phases, where k_r,k_ϕ,k_z are the radial, azimuthal and parallel components of the local Cartesian coordinate system in a cylindrical model, and the tilde above denotes a spatial harmonic of the Fourier transform. For example

$$\tilde{B}_r=\frac{1}{(2\pi)^{3/2}}\int d^3\mathbf{r}B_r(\mathbf{r})e^{-i\mathbf{kr}}.$$

Using the natural assumption that the ion Larmor radius ρ_i is small as compared to the wavelength $k_\perp\rho_i=k_\perp v_{Ti}/\omega_i\ll1$, where $v_{Ti}\sim v_\perp$ is ion thermal velocity, we obtain

$$D\approx\frac{\pi}{4}\frac{v_\perp^4}{B_0^2}\int d^3\mathbf{k}\left\langle\left|k_r\tilde{B}_r+k_\phi\tilde{B}_\phi\right|^2\right\rangle\delta(\omega-k_zv_\parallel)$$

for the diffusion coefficient.

Note that $E_2=0$ for the Alfven waves, while the B_r component of the SMS wave field is singular, and the B_ϕ component has a finite amplitude in the absence of dissipation on the resonance surface. From the solution of (9) we know the structure of the wave field harmonic of the form

$$\overline{B}_r(r,m,k_z,\omega)=\frac{1}{(2\pi)^{3/2}}\int B_r(r,t)e^{-i(k_zz+m\phi-\omega t)}\,d\phi\,dz\,dt.$$

Leaving only the singular B_r component of the magnetic field in the expression for the diffusion coefficient, it can be written as

$$D\approx\frac{\pi}{4}\frac{v_\perp^4}{v_\parallel B_0^2}\sum_{m=0}^{\infty}\int_0^\infty\left\langle\left|\nabla_r\overline{B}_r(r,m,k_z=\omega/v_\parallel,\omega)\right|^2\right\rangle d\omega.\tag{14}$$

Here the integrand δ function was used for integrating over k_z. Averaging is over the phases of the frequency harmonic, as well as over the azimuthal and parallel harmonics of the wave vector.

As the initial condition for solving (13), we use the Maxwell distribution function

$$f(v_\parallel,v_\perp)=\frac{n_0}{\pi^{3/2}v_{Ti}^3}\exp\left(-\frac{v_\parallel^2+v_\perp^2}{v_{Ti}^2}\right),$$

where n_0 is the plasma ion concentration, $v_{Ti}=\sqrt{2T_i/m_i}$ is the thermal velocity of plasma ions on the magnetic shell under consideration. This function describes the equilibrium plasma state in the absence of waves. Presumably, plasma takes on this state in the geomagnetic tail lobes during the substorm recovery phase.

As follows from the form of the diffusion coefficient (14), Eq. (13) does not change the dependence of the distribution function on $v_\perp$.

Integrating (13) over $v_\perp$, we obtain

$$\frac{\partial \overline{f}}{\partial t} \approx \frac{\partial}{\partial v_\parallel} \overline{D} \frac{\partial \overline{f}}{\partial v_\parallel}, \tag{15}$$

where

$$\overline{f}(v_\parallel) = \int_0^{2\pi} d\phi \int_0^\infty v_\perp f(v_\parallel, v_\perp)\, dv_\perp = \frac{n_0}{\sqrt{\pi} v_{Ti}} \exp\left(-\frac{v_\parallel^2}{v_{Ti}^2}\right), \tag{16}$$

$$\overline{D} = \frac{1}{\pi v_{Ti}^2} \int_0^{2\pi} d\phi \int_0^\infty v_\perp D e^{-v_\perp^2/v_{Ti}^2}\, dv_\perp$$
$$\approx \frac{\pi}{2} \frac{v_{Ti}^4}{v_\parallel B_0^2} \sum_{m=0}^{\infty} \int_0^\infty \left\langle \left| \nabla_r \overline{B}_r(r, m, k_z = \omega/v_\parallel, \omega) \right|^2 \right\rangle d\omega. \tag{17}$$

Multiplying (15) by $\overline{f}$ on the left and integrating over $v_\parallel$, we have

$$\frac{1}{2} \frac{\partial}{\partial t} \int_{-\infty}^{\infty} \overline{f}^2\, dv_\parallel \approx -\int_{-\infty}^{\infty} \overline{D} \left(\frac{\partial \overline{f}}{\partial v_\parallel}\right)^2 dv_\parallel. \tag{18}$$

Hence, if a new equilibrium state is reached ($\partial \overline{f}/\partial t = 0$) at the asymptotic $t \to \infty$, a "plateau" must appear in the distribution function ($\partial \overline{f}/\partial v_\parallel = 0$) in the intervals of $v_\parallel$ where $\overline{D} \neq 0$.

5. Calculation of velocity acquired by magnetospheric plasma due to its interaction with MHD waves in the magnetosheath

Consider the conditions under which the distribution function of magnetospheric plasma ions is modified under the impact of the MHD wave flux from the magnetosheath. Firstly, the intervals $v_\parallel$ where $\overline{D} \neq 0$ are determined by the presence of magnetosonic waves in the solar wind far from the magnetosphere (when $r \to \infty$). As follows from (10), the solar wind is a transparency region for magnetosonic waves ($\mathrm{Re}(k_r^2) > 0$) when $\omega_S^2 < \overline{\omega}_A^2 < \omega_{A1}^2$ and when $\overline{\omega}_A^2 < \omega_{A2}^2$. When $r \to \infty$ we have $\omega_{A1}^2 = 1$, $\omega_{A2}^2 = \beta^*$. The first of these conditions defines a very narrow range of admissible wave parameters so that we ignore its presence. From the second condition we find that the solar wind is transparent in the intervals of parallel wave numbers $k_z < \min(k_1, k_2)$ and $k_z > \max(k_1, k_2)$, where $k_{1,2} = \omega/v_{1,2}$, $v_1 = v_0 + S_w$, $v_2 = v_0 - S_w$. In our model of the medium the sound velocity in the magnetosheath $S_w = 177$ km/s. For solar wind plasma flows with $v_0 > 200$ km/s we have $v_1 > v_2 > 0$ and the solar wind is opaque when $0 < k_1 < k_z < k_2$. Considering the resonance conditions for plasma particles interacting with waves ($k_z = \omega/v_\parallel$), we find that the distribution function remains unchanged in the range $v_2 < v_\parallel < v_1$.

The presence of resonance surfaces for SMS waves in the geotail should also be taken into account. Given the local dispersion equation for the SMS waves $\omega^2 = k_z^2 C_S^2$, we have $C_{S\,\max} > |v_\parallel| > C_{S\,\min}$. In our model, the value $C_{S\,\min} \approx 8$ km/s is reached on the axis of the plasma cylinder, and $C_{S\,\max} \approx 2000$ km/s in the vicinity of the magnetopause. Thus, there are three areas where a "plateau" forms in the distribution function $\overline{f}$: $-C_{S\,\max} < v_\parallel < -C_{S\,\min}$, $C_{S\,\min} < v_\parallel < v_2$ and $v_1 > v_\parallel > C_{S\,\max}$. The area $C_{S\,\min} < v_\parallel < v_2$ corresponds to "downstream", while the two other areas to "upstream" FMS waves in the solar wind. The corresponding distribution of $\overline{f}(v_\parallel)$ is presented in Fig. 4.

The level of the plateau in each of these areas is determined by the condition that the total number of particles should remain the same and can be expressed by the following relation

$$\overline{f}_j = \int_{v_{\parallel\min}}^{v_{\parallel\max}} \overline{f}(v_\parallel)\, dv_\parallel \Big/ (v_{\parallel\max} - v_{\parallel\min}),$$

where $j = 1, 2, 3$ is the number of an area with a "plateau" (see Fig. 4), and the values $v_{\parallel\max,\min}$ correspond to the maximum and minimum value of the parallel velocity of particles in each of these intervals. Satisfying these relations provides for maintaining the balance of the total equilibrium pressure and, hence, for keeping the Alfven speed and sound velocity profiles in the plasma unchanged.

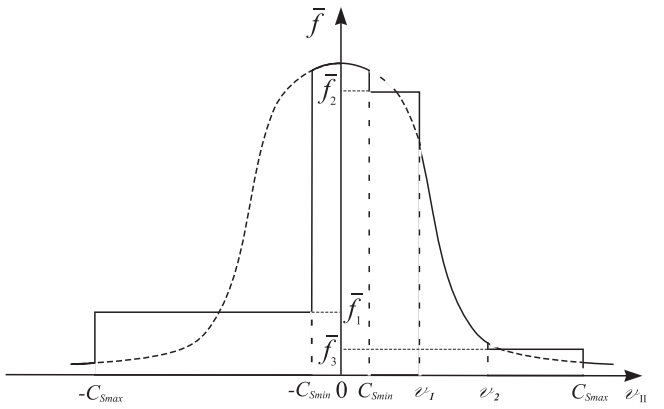

Fig. 4. "Plateau" formation on the plasma ion distribution function under the impact of MHD waves penetrating into the geotail lobes from the magnetosheath. The range $C_{S\,\min} < v_\parallel < v_1$ corresponds to the downstream FMS waves, and the ranges $-C_{S\,\max} < v_\parallel < -C_{S\,\min}$ and $v_2 < v_\parallel < C_{S\,\max}$ correspond to the upstream FMS waves in the magnetosheath.

The average velocity of plasma resulting from its interaction with MHD waves is determined by the equation

$$\overline{v}_0 = \frac{1}{n_0} \int_{-\infty}^{\infty} v_\parallel \overline{f}(v_\parallel)\, dv_\parallel.$$

Obviously, the contribution from symmetric (with respect to $v_\parallel = 0$) parts of $\overline{f}(v_\parallel)$ is zero. Fig. 5 shows the distribution of $v_0(r)$ calculated for the parameters of the cylindrical model of the geotail used in this study, for different solar wind velocities in the magnetosheath.

Fig. 5a presents the solar wind velocity $v_0(r)$ profiles taking into account the transition layer, and plasma velocity profiles in the geotail lobes $\overline{v}_0(r)$ calculated for two limiting cases. The first of these (curves 4 and 5 in Fig. 5a) assumes that all waves in the magnetosheath move "downstream" and plateau do not form in the ranges $-C_{S\,\max} < v_\parallel < -C_{S\,\min}$ and $v_1 > v_\parallel > C_{S\,\max}$. Obviously, in this case the impulse transferred by MHD waves to ions in the geotail lobes is tailward $\overline{v}_0(r) > 0$. In the second limiting case, the "downstream" and "upstream" fluxes of waves are equal. It is evident from Fig. 5a, that in this case the impulse transferred to plasma ions is Earthward. From satellite observations of solar wind oscillations, it is difficult to determine which portion of the wave flux is "downstream" or "upstream".

The most probable seems to be an intermediate case between the two, when the "downstream" waves in the magnetosheath occupy a broader part of the spectrum than do the "upstream" waves. The summarized plasma velocity distribution $v_0(r) + \overline{v}_0(r)$ in the case when the "upstream" waves are absent from the range $-C_{S\,\max} < -300$ km/s $< v_\parallel < -C_{S\,\min}$ is presented in Fig. 5b. Evidently, in this case the impulse transferred to ions in the regions adjacent to the transition layer reverses the plasma flow motion back to Earth, whereas closer to the cylinder axis the motion becomes tailward again. Note that the model in question is inapplicable to those inner parts of the geotail where the plasma sheet lies. As will be seen later, another reason why the obtained results cannot be used for the inner regions of the geotail is that the characteristic time for the asymptotic regime of the plasma flow to set in there is too long.

6. Calculation of the characteristic time needed for the asymptotic regime to set in the plasma flow

The profile calculations of plasma velocity acquired under the influence of MHD waves in the previous section do not depend on

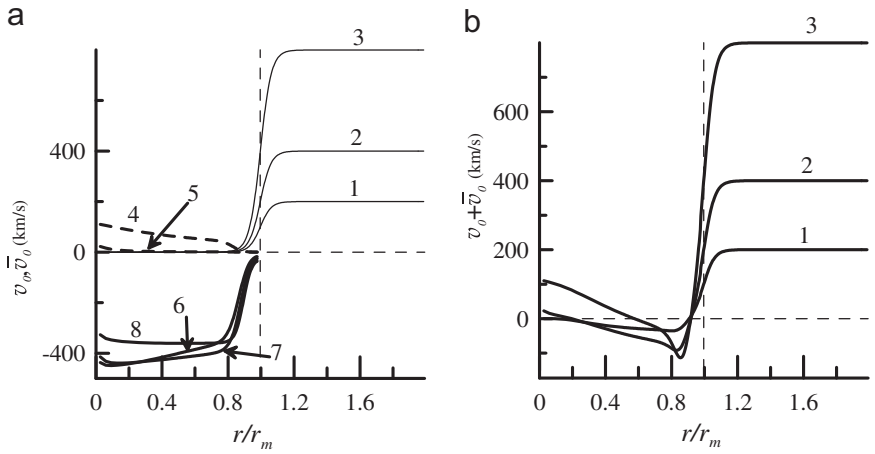

Fig. 5. Distribution over the radius of the plasma flow velocities v_0 in the magnetosheath and magnetospheric convection velocity $\bar{v}_0$ for different velocities of the solar wind. Curves 1–3 in panel (a) correspond to the solar wind velocity distribution for $v_0 = 200, 400, 800$ km/s, curves 4 and 5 are the magnetospheric convection velocities when $v_0 = 400, 800$ km/s, in the absence of "upstream" FMS waves in the magnetosheath, and curves 6–8 ($v_0 = 200, 400, 800$ km/s) are the magnetospheric convection velocities for equal fluxes of "downstream" and "upstream" FMS waves in the magnetosheath. Panel (b) shows the distribution of complete velocity $v_0 + \bar{v}_0$ (curves 1–3 for $v_0 = 200, 400, 800$ km/s) when the flux of "downstream" FMS waves prevails over that of the "upstream" FMS waves in the magnetosheath.

their amplitude. This is due to the fact that the flow velocity to be calculated corresponds to the asymptotic regime at $t \to \infty$. The real magnetospheric plasma flow, however, takes a finite interval of time to set in. The characteristic time τ needed for the completely motionless plasma to switch to the asymptotic regime of its motion is determined by the amplitude of MHD waves transferring the momentum from the solar wind into the magnetosphere. To estimate this time, let us replace the time derivative in (18) with τ^{-1}, resulting in

$$\tau \approx 2 \int_{-\infty}^{\infty} \bar{f}^2 \, dv_{\parallel} \Big/ \int_{-\infty}^{\infty} \bar{D} \left(\frac{\partial \bar{f}}{\partial v_{\parallel}} \right)^2 dv_{\parallel}. \tag{19}$$

For the $\bar{f}$ function, let us choose the Maxwell distribution of form (16).

To calculate the diffusion coefficient $\bar{D}$, it is necessary to specify the spectrum of MHD waves in the magnetosheath. There are many onboard observations of variations in the solar wind parameters. They are generally stochastic oscillations with a "white noise" spectrum (Matthaeus and Goldstein, 1982). Two types of statistical observations of these spectra are cited in the literature. A number of works present oscillation energy density spectra depending on frequency (Marsh and Tu, 1990; Klein et al., 1993). According to these data, oscillation energy $W(\omega)$ can be approximated by a power function of the form $W \sim \omega^{-\alpha}$ in a greater part of the frequency range. The exponent α is in the range $1 \lesssim \alpha \lesssim 3$ with an average of $\alpha = 5/3$, which corresponds to Kolmogorov's spectrum for well-developed turbulent oscillations. When frequency $\omega > \omega_i$, where ω_i is the gyrofrequency of solar wind ions, the spectrum of $W(\omega)$ drops sharply due to a resonant ion-cyclotron absorption of waves.

Other papers (see Goldstein et al., 1995) present data on the oscillation spectrum of solar wind plasma concentration as a function of wavelength, i.e. in effect, the function $\langle n(k_t) \rangle$, where $k_t = \sqrt{\bar{k}_z^2 + m^2/\bar{r}^2}$ is the tangential component of the wave vector, $\bar{k}_z$ is the parallel component of the wave vector in the reference frame moving at the solar wind velocity, $\bar{r}$ is the radius of the cylindrical model for which the oscillation spectrum is set (our calculations assumed $\bar{r} = 2r_m$). These observations imply that the spatial spectrum can be approximated by a function of the form $\langle n(k_t) \rangle \sim k_t^{-\beta}$, where $\beta \approx 5/3$.

Since the oscillation energy density is a quadratic function of the oscillation amplitude, the following modeling expression may be suggested for the spectrum of magnetic field oscillations of the solar wind

$$\langle |\bar{B}_r|^2 \rangle = C \Phi(k_t, \omega) \omega^{-\alpha} k_t^{-2\beta}, \tag{20}$$

where C is a constant determined by the average oscillation amplitude, and $\Phi(k_t, \omega)$ is a step function determining the upper and lower limits of the spectrum, as well as the wave range for which the solar wind is an opacity region. The spectrum (20) should be cut off when $\omega \to 0$. It is known from Matthaeus and Goldstein (1982) that there is a maximum correlation scale $\hat{l} \sim 150 R_E$ related to the inhomogeneous structure of the solar wind. It is possible to introduce minimum frequency $\hat{\omega} = 2\pi v_0/\hat{l}$ limiting the oscillation frequency range from below. Then the function $\Phi(k_t, \omega)$ may be written as

$$\Phi(k_t, \omega) = \Theta(\omega - \hat{\omega}) \Theta(\omega_i - \omega) [\Theta(\bar{k}_z - \bar{k}_2) + \Theta(\bar{k}_1 - \bar{k}_z)],$$

where $\Theta(x)$ is the Heaviside step function, and $\bar{k}_1 = -\omega/S_w < \bar{k}_z < \bar{k}_2 = \omega/S_w$ is the range of parallel wave numbers corresponding to solar wind opacity for FMS waves. Constant C in (20) is determined by the inverse Fourier-transformation

$$\langle |B_r|^2 \rangle = \frac{1}{(2\pi)^{3/2}} \sum_{m=0}^{\infty} \int_0^{\infty} d\omega \int_{-\infty}^{\infty} \langle |\bar{B}_r|^2 \rangle \, d\bar{k}_z$$

$$= \frac{C}{(2\pi)^{3/2}} \sum_{m=0}^{\infty} \int_0^{\infty} \omega^{-\alpha} \, d\omega \int_{-\infty}^{\infty} \Phi(k_t, \omega) k_t^{-2\beta} \, d\bar{k}_z,$$

where $\langle |B_r|^2 \rangle$ is the mean square of the amplitude of the B_r component of the solar wind oscillation field at $r = \bar{r}$. In our calculations we assume $\langle |B_r| \rangle \sim 0.2 B_0 \approx 1$ nT. Fig. 6 shows the distribution over the radius of the characteristic time τ needed for the asymptotic regime to set in the geotail plasma flow, as calculated by formula (19), in which the diffusion coefficient is determined by (17), and the spectrum of FMS fluctuations in the magnetosheath (20) corresponds to the plasma flow profiles in Fig. 5b. It is evident that the values of τ comparable with the time during which the geotail can be regarded as a fairly stable plasma configuration (average interval between two successive substorms ~ 3–6 h) is achieved in the ranges $0.8 r_m < r < r_m$ (for the $v_0 = 400$ km/s solar wind) and $0.85 r_m < r < r_m$ (for the $v_0 = 200, 800$ km/s solar wind). It is in this range of magnetic shells that a maximum concentration of resonance surfaces for SMS waves is reached in our model geotail.

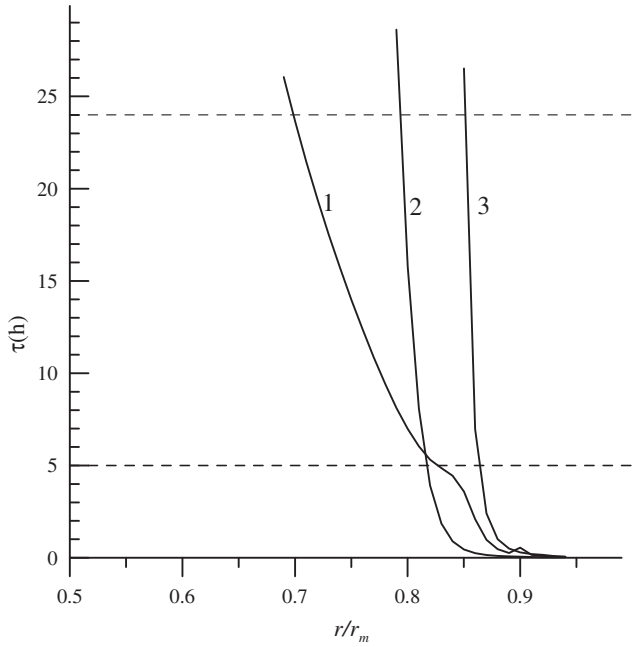

Fig. 6. Distribution over the radius of the characteristic time τ needed for the asymptotic regime of the magnetospheric convection to set in for different solar wind velocities in the magnetosheath. Curves 1–3 correspond to $v_0 = 200, 400, 800$ km/s for an average amplitude of stochastic FMS oscillations in the magnetosheath $\langle |B_r| \rangle \sim 1$ nT.

The obtained values of τ can be regarded as the upper bound of the time needed for the asymptotic regime to set in the plasma flow. Time τ decreases quadratically when the amplitude of turbulent plasma oscillations in the magnetosheath increases. Moreover, a more accurate approach to solving the initial problem (15) must take into account contribution from MHD oscillations related to the evolution of a Kelvin–Helmholtz instability at the magnetopause. The solar wind being opaque for such oscillations (see Leonovich, 2011a,b), the problem would be formulated in a different manner than in this work. If the flux of unstable waves in the geotail is assumed to be comparable with that considered in this work, we may expect a 2–3-fold decrease in the characteristic time τ as well as a somewhat wider range of magnetic shells on which the asymptotic regime of magnetospheric convection can set in.

7. Conclusion

Let us list the main results of this work.

1. The spatial structure of monochromatic MHD waves was calculated in a cylindrical model of the geotail the plasma distribution in which is typical of the tail lobe. It is shown that there is a rather wide (in frequency and wave numbers) range of waves for which the conditions for magnetosonic resonance are satisfied in the geotail. The highest concentration of resonance shells is achieved in the geotail regions adjacent to the magnetopause.
2. In the framework of quasilinear theory, an approximate solution is obtained to Eq. (15), describing the evolution of the plasma ion distribution function under the impact of an MHD wave flux. It is shown that, on the time asymptotic (when $t \to \infty$), an Earthward plasma flow moving at 50–150 km/s is established in the geotail lobe regions adjoining the magnetopause.
3. The characteristic time τ needed for the asymptotic regime to set in the plasma flow is calculated for the average amplitude ~ 1 nT of FMS oscillations in the magnetosheath and for a spectrum typical of well-developed turbulent oscillations. In the regions adjoining the magnetopause, the time τ was found to be comparable with the mean time interval between two successive substorms $\sim 3-6$ h, during which the geotail configuration can be regarded as stable, but increased sharply on the inner magnetic shells. Such interaction is most effective for solar wind of an average velocity $v_0 \sim 400$ km/s for which the interval of magnetic shells with $\tau < 5$ h extends to $r \approx 0.8 r_m$.

Thus, we conclude that the FMS wave flux moving from the magnetosheath onto the magnetopause transfers a momentum to plasma ions in the geotail lobes which is capable of forming an Earthward flow of magnetospheric convection. This process is most effective in the region of open field lines adjoining the magnetopause, where the concentration of resonance shells for SMS waves is highest. This mechanism may explain the formation of an Earthward flow of magnetospheric convection in the geotail lobes (on open field lines) during prolonged periods of the Northern IMF component.

Acknowledgments

This work was partially supported by RFBR Grant # 12-02-00031 and by Program of presidium of Russian Academy of Sciences # 22.

References

Akhiezer, A.I., Akhiezer, I.A., Polovin, R.V., Sitenko, A.G., Stepanov, K.N., 1979. In: Plasma Electrodynamics. Nauka, Moscow, pp. 461. (in Russian).

Axford, W.I., Hines, C.O., 1961. A unifying theory of high-latitude geophysical phenomena and geomagnetic storms. Canadian Journal of Physics 39, 1433–1464.

Borovsky, J.E., Thomsen, M.F., Elphic, R.C., Cayton, T.E., McComac, D.J., 1998. The transport of plasma sheet material from the distant tail to geosynchronous orbit. Journal of Geophysical Research 103, 20297–20331.

Cowley, S.W.H., 1983. Interpretation of observed relations between solar wind characteristics and effects at ionospheric altitudes. In: Hultqvist, B., Hagfors, T. (Eds.), High-latitude Space Plasma Physics. Plenum Press, New York/London, pp. 225–249.

Crooker, N.U., Lyon, J.G., Fedder, J.A., 1998. MHD model merging with IMF by: lobe cells, sunward polar cap convection, and overdraped lobes. Journal of Geophysical Research 103, 9143–9152.

Dungey, J.W., 1961. Interplanetary magnetic field and the auroral zones. Physical Review Letters 6, 47–48.

Forster, M., Haaland, S.E., Paschmann, G.J., Quinn, M., Torbert, R.B., Vaith, H., Kletzing, C.A., 2008. High-latitude plasma convection during Northward IMF as derived from in-situ magnetospheric Cluster EDI measurements. Annales Geophysicae 26, 2685–2700.

Goldstein, M.L., Roberts, D.A., Matthaeus, W.H., 1995. Magnetohydrodynamic turbulence in the solar wind. Annual Review of Astronomy and Astrophysics 33, 283–325.

Klein, L., Bruno, R., Bavassano, B., Rosenbauer, H., 1993. Anisotropy and minimum variance of magnetohydrodynamic fluctuations in the inner heliosphere. Journal of Geophysical Research 98, 17461–17469.

Kozlov, D.A., 2010. Transformation and absorption of magnetosonic waves generated by solar wind in the magnetosphere. Journal of Atmospheric and Solar-Terrestrial Physics 72, 1348–1353.

Leonovich, A.S., Mishin, V.V., Cao, J.B., 2003. Penetration of magnetosonic waves into the magnetosphere: influence of a transition layer. Annales Geophysicae 21, 1083–1093.

Leonovich, A.S., Kozlov, D.A., 2009. Alfvenic and magnetosonic resonances in a nonisothermal plasma. Plasma Physics and Controlled Fusion 51, 085007. doi:10.1088/0741-3335/51/8/085007.

Leonovich, A.S., 2011a. MHD-instability of the magnetotail: global modes. Planetary and Space Science 59, 402–411.

Leonovich, A.S., 2011b. A theory of MHD instability of an inhomogeneous plasma jet. Journal of Plasma Physics 77, 315–337.

Marsh, E., Tu, C.-Y., 1990. Spectral and spatial evolution of compressive turbulence in the inner solar wind. Journal of Geophysical Research 95A, 11945–11956.

Matthaeus, W.H., Goldstein, M.L., 1982. Measurement of the rugged invariants of magnetohydrodynamics turbulence in the solar wind. Journal of Geophysical Research 87A, 6011–6028.

Mazur, V.A., Leonovich, A.S., 2006. ULF hydromagnetic oscillations with the discrete spectrum as eigenmodes of MHD-resonator in the near-Earth part of the plasma sheet. Annales Geophysicae 24, 1639–1648.

Mishin, V.V., 2005. Velocity boundary layers in the distant geotail and the Kelvin–Helmholtz instability. Planetary and Space Sciences 53, 157–160.
Miura, A., 1984. Anomalous transport by magnetohydrodynamic Kelvin–Helmholtz instabilities in the solar wind-magnetosphere interaction. Journal of Geophysical Research 89, 801–818.
Ponomarev, E.A., Sedykh, P.A., Urbanovich, V.D., 2006. Generation of electric field in the magnetosphere, caused by processes in the bow shock. Journal of Atmospheric and Solar-Terrestrial Physics 68, 679–684.
Potemra, T.A., Zanetti, L.J., Bythrow, P.F., Lui, A.T.Y., Iijima, T., 1984. B_y-dependent convection patterns during northward interplanetary magnetic field. Journal of Geophysical Research 89, 9753–9760.
Ruohoniemi, J.M., Baker, K.B., 1998. Large-scale imaging of high-latitude convection with Super Dual Auroral Radar Network HF radar observations. Journal of Geophysical Research 103, 20797–20811.
Sandholt, P.E., Farrugia, C.J., Cowley, S.W.H., Lester, M., Denig, W.F., Cerisier, J.C., Milan, S.E., Moen, J., Trondsen, E., Lybekk, B., 2000. Dynamic cusp aurora and associated pulsed reverse convection during northward interplanetary magnetic field. Journal of Geophysical Research 105, 12869–12894.
Sergeev, V.A., Pellinen, R.J., Pulkkinen, T.I., 1996. Steady magnetospheric convection: a review of recent results. Space Science Reviews 75, 551–604.
Sergeev, V.A., Tsyganenko, N.A., 1980. The Earth's Magnetosphere. Moscow, Nauka (in Russian).
Sizonenko, V.L., Stepanov, K.N., 1968. Quasilinear theory of plasma oscillations with linear dispersion Ukrainian. Journal of Physics 13, 876–878.
Vasyliunas, V.M., 2001. Electric field and plasma flow: what drives what? Geophysical Research Letters 28, 21772180.